Bandwidth enhancement of 2-D leaky-wave antennas with double-layer periodic surfaces

Mateo-Segura, Carolina; Feresidis, Alexandros P.; Goussetis, George

DOI:
10.1109/TAP.2013.2292076

Bandwidth Enhancement of 2-D Leaky-Wave Antennas with Double-Layer Periodic Surfaces

Carolina Mateo-Segura, *Member, IEEE*, Alexandros P. Feresidis, *Senior Member, IEEE* and George Goussetis, *Member, IEEE*

***Abstract*— Broadband high-gain 2-D Fabry-Perot (FP) Leaky-Wave Antennas (LWAs) consisting of two periodic metallodielectric arrays over a ground plane are presented. Full-wave method of moments (MoM) is employed for the estimation of the near fields upon plane wave illumination and the extraction of the far field directivity and radiation patterns of the LWA. This yields a fast and rigorous tool for the characterization of this type of antennas. Qualitative design guidelines to tailor the antenna directivity bandwidth are provided for the first time based on a detailed analysis of the excited modes. Numerical examples are given to demonstrate the technique and prove the improvement in the antenna bandwidth. The proposed antenna exhibits a six-fold bandwidth improvement compared with the single array LWA with the same directivity. Simulated and experimental results from a finite size antenna prototype are presented.**

***Index Terms* — periodic surfaces, Leaky-Wave antennas (LWAs), Broadband antennas, High directive antennas.**

I. Introduction

HIGHLY directive two dimensional Fabry-Perot cavity type Leaky Wave antennas have received significant research interest in the last few years. They provide numerous advantages such as low complexity feeding network, high efficiency and compatibility with established manufacturing technologies [1-17]. In these antennas, the cavity resonance increases the directivity of a single radiating source positioned in the cavity (Fig. 1). The higher directivity typically results in a narrower bandwidth which is a disadvantage in modern communication systems. Therefore, the design of high-gain FP LWAs, which also exhibit a broad bandwidth performance, remains a significant challenge.

Different approaches have been adopted to overcome the bandwidth limitation. Recently, the authors of [18-20] replaced the single feed by a sparse array feed increasing the radiating aperture size and thus widening the bandwidth of the antenna for a fixed gain value. However, this design adds complexity in the antenna implementation due to the multiple feeds. Tapered-size partially reflective surfaces (PRSs) and artificial magnetic conductors have also been employed with the same purpose [21, 22]. In [10], a condition was derived for the PRS in single-feed FP antennas to exhibit a reflection phase increasing with frequency in order to achieve wide bandwidth. More recently, an optimised broadband FP antenna design with compact lateral dimensions and lateral cavity walls has been reported in [23]. The design was based on a double-layer metallo-dielectric PRS with different array element size (i.e. arrays with dissimilar reflectivity). The double-layer array configuration provided a reflection phase response that increased almost linearly with frequency within a frequency range. As a result, the resonance condition of the cavity was satisfied over a wider range of frequencies thus increasing the antenna bandwidth. Subsequently, two-layer PRS arrays have also been employed for bandwidth enhancement of FP antennas in other interesting configurations [24-27]. Nevertheless, a detailed design procedure for bandwidth enhancement of FP LWAs has yet to be presented. Moreover, the modes excited within double-layer PRS FP cavity antennas have not been studied in detail [28-30].

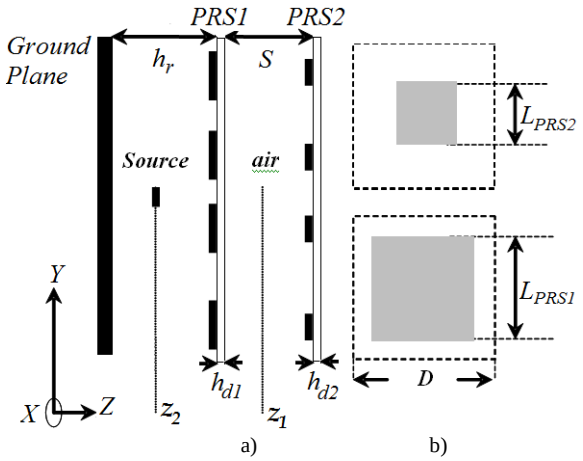

Fig. 1 Cross-section of a) double layer free-standing dipole PRS Leaky-Wave Antenna and b) unit cell dimensions of the double layer dipole PRS.

In this paper, we present for the first time a qualitative design and experimental validation of broadband 2-D periodic FP LWAs based on optimised double-layer PRSs. Using full-wave spectral domain periodic analysis together with

Manuscript received December, 2012. C. Mateo-Segura and A. P. Feresidis acknowledge the support by MRC-EPSRC-BBSRC under Grant G0802609. G. Goussetis wishes to acknowledge the support by the Royal Academy of Engineering under a five-year research fellowship.

C. Mateo-Segura is with the School of Engineering and Physical Science, Heriot Watt University, Edinburgh EH14 4AS, UK (e-mail: c.mateo@ieee.org).

A.P. Feresidis is with the School of Electronic Electrical and Computer Engineering, University of Birmingham, Birmingham, B15 2TT, UK. (e-mail: a.feresidis@bham.ac.uk).

G. Goussetis is with the Institute of Electronics Communications and Information Technology (ECIT), Queen's University Belfast, Northern Ireland, BT3 9DT, UK (e-mail: G.Goussetis@ieee.org).

reciprocity [12-13, 31-32], we demonstrate that a two-cavity antenna provides increased bandwidth as a result of coupling the modes associated with either cavity. Subsequently, we investigate the directivity, radiation bandwidth and patterns of LWAs composed of double layer two-dimensional periodic arrays acting as PRSs over a ground plane, as shown in Fig. 1. The modes excited in the FP cavities of the antenna are carefully examined following a qualitative parametric study. An optimal finite size LWA is simulated using CST Microstripes and subsequently fabricated in order to validate the accuracy of the design method. The gain and principal plane radiation patterns are measured and compared to those obtained from full-wave simulations.

II. Periodic Analysis of Double Layer PRS Antenna

In [23], a simple ray optics analysis was used to design a double layer LWA with broadband response based on the optimization of the double layer PRS [10]. In this section, a full wave analysis is employed instead [32]. Let us consider a working example consisting of a lower square patch PRS array (*PRS1*) with dimensions, L_{PRS1}=10.7mm within a square unit cell of D=11mm and an upper square patch PRS array (*PRS2*), with dimensions L_{PRS2}=6mm within the same unit cell. The arrays are considered to be printed on a 1.6mm thick dielectric substrate with dielectric constant 4.2 and loss tangent 0.025 at 14GHz (i.e. characteristics of the FR-4 employed in the fabrication) and separated by a distance S=9.5mm (Fig. 1). Periodic MoM is used to calculate the reflection coefficient, magnitude and phase and is shown in Fig. 2a. A minimum reflection magnitude appears at 14.2 GHz. The reflection phase increases with frequency in the vicinity and in particular in the range between 13.9 GHz and 14.5 GHz. Therefore, according to the conclusions of [23], broadband LWA directivity would be expected within this frequency range. To prove this, the FP-LWA is subsequently formed by placing the double-layer PRS above a ground plane at distance h_r, estimated by a ray optics approximation [9]. The value of h_r was chosen at approximately 10.7 mm so that the theoretical optimum PRS phase obtained from ray analysis (Fig. 2a) matches the reflection phase of the double layer PRS within the frequency range.

In the following, the technique introduced in [12, 32] is employed for the analysis of the FP-LWA under investigation. A full-wave periodic spectral domain MoM analysis of the antenna unit cell is carried out and the excited near field within the antenna cavities, at $z_1 = S/2$ and $z_2 = h_r/2$, is sampled. By reciprocity, the far field radiation performance of the antenna is obtained, under the assumption of a Hertzian dipole excitation at the centre of the lower cavity (i.e. z_2) [32]. For the estimated value of h_r, the directivity and power density are calculated as in [32]. The power density radiated at broadside ($\propto |E|^2$) by the double layer LWA with a y-polarized point source with unit electric field amplitude (V/m) at z_2 is depicted in Fig. 2b, expressed in dB and normalized to 1 W/m^2. The 3-dB *radiation bandwidth* at broadside, marked with a blue arrow in Fig. 2b, is defined as the frequency range where the power density level radiated at broadside is within 3dB of its maximum, thus 6%. In order to obtain the directivity exploiting reciprocity, this value should be normalized against the integral of the power density for all possible angles of incidence [32]. This value can be estimated using MoM and reciprocity arguments after extracting the 3-D radiation performance and represents the total power radiated to all directions when excited by an ideal polarised source at the observation point, P_{rad}. The directivity at broadside is also presented in Fig. 2b with a black line while P_{rad} is superimposed in red. As shown, although the radiation bandwidth increases significantly when compared to common single layer FP LWA [1, 9-17], the directivity bandwidth increases only slightly. The directivity curve shows a maximum value at 13.85 GHz, which smoothly decreases with frequency up to 14.5 GHz; beyond that point, the directivity drops rapidly.

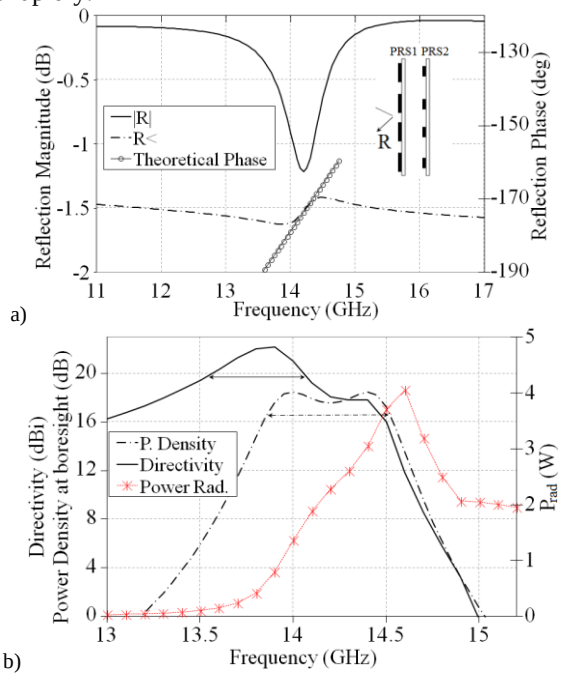

Fig. 2 a) Reflection coefficient (normal plane wave impinging PRS1) as obtained using MoM. The optimum phase is also calculated using ray optics. and b) Directivity and power density radiated at boresight by the LWA excited by a y-polarised Hertzian dipole at z_2. The total radiated power by the antenna is also plotted.

The reduced directivity bandwidth can be explained by the variation of the total radiated power by the antenna, $P_{rad,}$ with frequency. As shown, a significant reduction of the radiated power is observed at low frequencies. This is due to the fact that at low frequencies the resonant leaky odd mode of the cavity is close to and eventually below cut-off and thus weakly excited; the fields below cut-off are evanescent and are concentrated in the near-field region of the antenna. Due to the inverse relation between total power radiated and directivity, the low values of the power radiated cause the directivity to be higher at low frequencies thus altering the flat broadband response of the power density. Thus, ray optics provides a good starting point design for broadband antennas albeit further optimizations are still required.

A. *Near-Field analysis and modes excited in the LWA*

In order to improve the directivity bandwidth of the antenna, the excited near fields are carefully examined. In particular, the magnitude and phase of the *y*-component of the electric near field excited at the centre of the two cavities of the LWA (i.e. z_1, z_2 in Fig. 1) under normal plane wave illumination is calculated and depicted in Fig. 3. A null of the field at z_1 appears at 14.2 GHz which also corresponds to the point of minimum reflection (see Fig. 2a). Two peaks on either side of the null indicate two resonances associated with this structure. Observing the phase of the fields, the lower frequency resonance is attributed to an *odd mode* (fields π-rad out of phase, antiparallel fields) while the higher frequency to an *even mode* (in phase, parallel fields). The emergence of even and odd modes in coupled resonator structures is commensurate to coupled resonant cavity structures, such as those encountered in distributed RF filters [33]. In light of this observation, in the remaining we present a study of the modes excited in the antenna of Fig. 1.

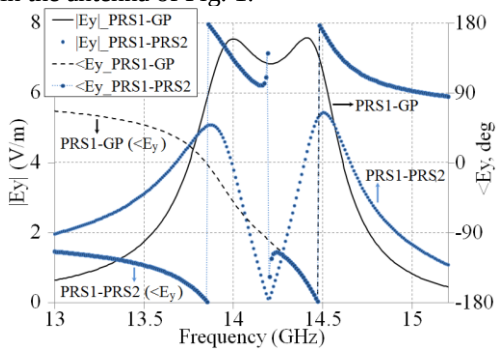

Fig. 3 Magnitude and phase of the y-component of the excited electric near-field at z_1 and z_2 when a GP is placed at h_r=10.7 mm.

For a uniform LWA the dispersion of the leaky mode is inherently linked with the direction of maximum directivity; in particular the phase constant (β) of the leaky mode is proportional to sin(θ), where θ is the angle of incidence relative to the *Z*-axis, Fig. 1. Therefore, the evolution of the modal properties can be understood by studying the directivity of the antenna for different angles, θ, and frequencies. The study is based on the dimensions of the antenna in Fig. 2. For the sake of brevity, only the E-plane is considered here, which corresponds to TM leaky modes [32]. Similar graphs and conclusions can be extracted for the H-plane and TE leaky modes. Without loss of generality and in order to simplify the study, no dielectric support is taken into consideration. Moreover, with reference to Fig.1, we set h_r=*S*=10.7 mm, which in the absence of external reactive loading from PRS2 suggests that the two cavities are synchronously tuned [33]. The latter condition is valid when the external coupling to the coupled resonator system is weak; this is the case of a very reflective PRS2, which here is imposed by setting L_{PRS2}=10.99mm. Under these conditions, the directivity as a function of the angle for various frequencies and different values of L_{PRS1} is plotted in Fig. 4.

As shown, in the case of a very reflective PRS1, (L_{PRS1}=10.99mm), the line of directivity maxima is unique indicating that a single TM mode is associated with the two cavity structure. This is attributed to the very high reflectivity of PRS1, which suggests that the two cavities are very weakly coupled; in accordance to the case of two weakly-coupled synchronously tuned resonators, the split of modes to even and odd is not observed. Instead, and since the leakage of the antenna is very small, the dispersion of the TM modes in the two cavities resembles the dispersion of a parallel plate waveguide with the same dimensions, which is superimposed in Fig. 4a with a dash black line. The two resonators are isolated and support uncoupled TM modes with cut-off frequency at around 14GHz given by Eq. 1

$$k_c = \frac{m\pi}{h_r} \tag{1}$$

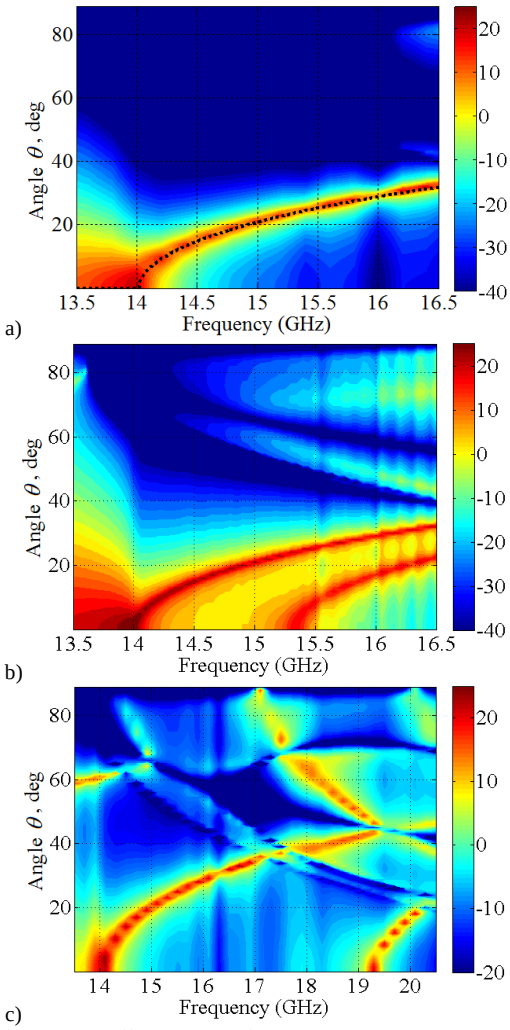

Fig. 4 Directivity at different angles for the synchronous cavity excited by a unit amplitude electric line source located at z_2 when a GP is placed at h_r=10.7 mm, *S*=h_r, L_{PRS2}= 10.99 mm and L_{PRS1} a) 10.99mm, b) 10mm and c) 5mm.

As the reflectivity of PRS1 reduces the modes associated with the two cavities are increasingly coupled; coupled mode theory [33] predicts that the frequency split to odd and even modes increases as the level of coupling increases. This is observed in Fig. 4b, 4c, which show the cut-off frequency of the odd and even modes at f_{odd} = 14GHz and f_{even}=15.8GHz and f_{odd} = 14GHz and f_{even}=19.3GHz respectively. It is noted that the phase plots associated with Fig. 4 have been obtained (are not shown here for brevity) and are commensurate with the use of the terms odd and even. Secondary maxima are observed at about 60° for high frequencies, these are grating lobes of the periodic PRS1 employed (*D*=11mm). It is further

noted that for the case of synchronously tuned resonators, the split of the cut-off frequencies between the even and odd mode is related to the coupling coefficient, *k*, using [33]

$$k = \frac{f_{even}^2 - f_{odd}^2}{f_{even}^2 + f_{odd}^2} \quad (2)$$

Further investigations in this direction that can potentially lead to a deterministic design of multilayer FP antennas will be the aim of a future paper.

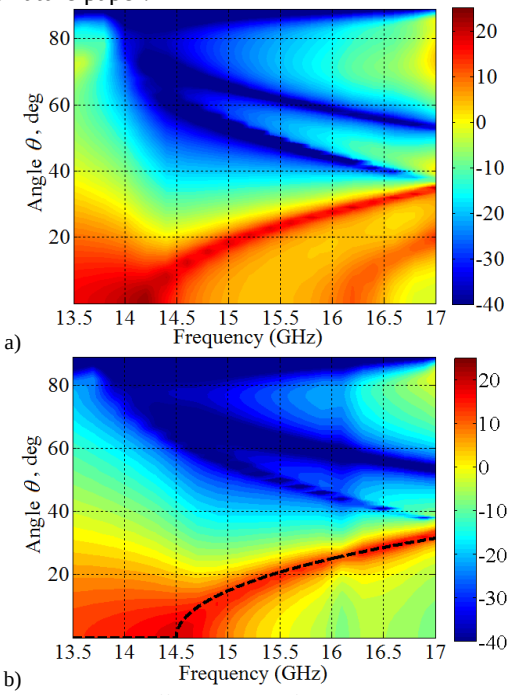

Fig. 5 Directivity at different angles for the cavity excited by a unit amplitude electric line source located at z_2 when a GP is placed at h_r=10.7 mm, S=h_r, L_{PRS1}= 10 mm and L_{PRS2} is a) 9mm, and b) 5mm.

Next, we investigate the effect of varying L_{PRS2} for L_{PRS1}=10mm. Coupled resonator theory suggests that introducing external coupling will reactively load the resonator formed between PRS1 and PRS2, so that the synchronously tuned assumption is no longer valid. For asynchronous coupled resonators other appropriate formulas are employed on the calculation of the coupling coefficient (3) where f_{r2} and f_{r1} are the resonant frequency of each cavity resonator [33].

$$k = \pm\frac{1}{2}\left(\frac{f_{r2}^2 + f_{r1}^2}{f_{r2}\,f_{r1}}\right)\sqrt{\left(\frac{f_{even}^2 - f_{odd}^2}{f_{even}^2 + f_{odd}^2}\right)^2 - \left(\frac{f_{r2}^2 - f_{r1}^2}{f_{r2}^2 + f_{r1}^2}\right)^2} \quad (3)$$

As the reflectivity of *PRS2* reduces (L_{PRS2}=9mm in Fig. 5a) the cut-off frequency of both modes appears at higher frequencies (f_{odd} = 14.2GHz and f_{even}=16.2GHz) and the even mode resonance becomes less evident; as the transparency of *PRS2* increases (L_{PRS2}=5mm in Fig. 5b) the resonance in the cavity formed by PRS1 and PRS2 becomes weaker and the modal characteristics become similar to that of the single layer PRS1 LWA or equivalently a parallel plate waveguide with dimensions h_r=10.3mm.

In the context of asynchronously tuned cavities, we also investigate the effect of modifying the distance between the two periodic arrays, *S*. The directivity at boresight vs. frequency for different values of *S*, when L_{PRS1}=10.7mm, L_{PRS2}=6mm and h_r=10.7mm is presented in Fig. 6. Reducing the distance between the two arrays results in a stronger excitation of the odd mode (peak at lower frequency) and a weaker excitation of the even mode (peak at higher frequency). The peak of the odd mode moves slightly towards higher frequency values and becomes sharper, due to the higher reflectivity values of the individual patch array at higher frequencies. The contrary happens if *S* increases. Larger *S* values further lead to wider separation between the odd and even mode response. It is instructive to note that all curves of Fig. 6 cross at the same point; the corresponding frequency coincides with a field null between the two PRS arrays, Fig. 3 (also the minimum reflectivity point in Fig. 2a) and, as expected, this frequency point is not affected by the distance between the two arrays.

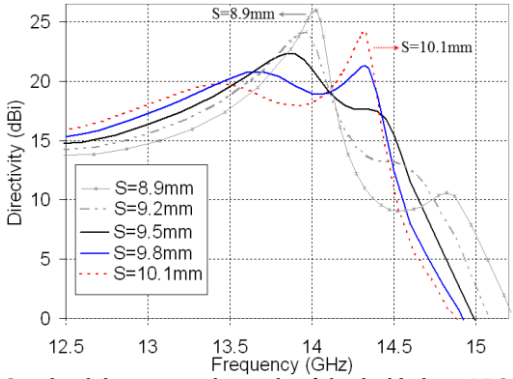

Fig. 6 Simulated directivity at boresight of the double-layer PRS LWA for varying distance between the PRS arrays, *S*, obtained using full-wave MoM.

B. Optimized double layer LWA

In view of the modal characteristics of the double layer LWA discussed above, a design offering broadband operating frequency with reduced directivity ripple has been numerically optimized. The directivity of the optimized design at various angles and frequencies is depicted in Fig. 7a and b, for H-plane (TE mode) and E-plane (TM mode) respectively. Both PRSs are printed on dielectric substrates as in Fig. 2 to allow for a rigid fabricated antenna prototype. The square unit cell edge is *D* = 11mm for both arrays. The square patch edge of PRS2 is L_{PRS2}=5.0 mm whilst for PRS1 is L_{PRS1}=10 mm (Fig. 1). The separation distance of the two dielectric boards is *S* =10.1 mm. The two boards are separated by air and located on top of a ground plane at distance h_r=10.9 mm. The power density radiated at boresight as a function of the frequency is shown with black dash line with triangle marker in Fig. 8. It proves a stronger excitation of the even mode, which compensates the increased power radiated by the antenna at higher frequencies. The 3dB directivity bandwidth at broadside as obtained by full-wave MoM for infinite arrays, (Fig. 8 with a dash blue line) is over 11% with a maximum directivity of 20.2dBi and a ripple of less than 2 dBi. For comparison, the 3dB directivity bandwidth of a single layer patch PRS LWA with the same directivity, 20.2dBi at 14GHz, on the same substrate, and with dimensions L_{PRS}= 8.5 mm, *D*=11 mm and h_r=9.2 mm is 1.65% which shows a directivity bandwidth enhancement by a factor of six for the double layer PRS FP LWA with an ideal source. As a note, dual-band LWA can be achieved using the proposed approach.

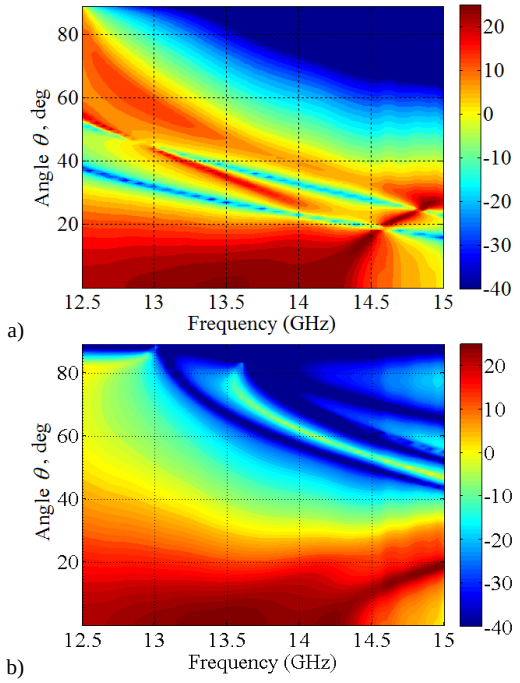

Fig. 7 Directivity of the a) H- plane (φ=0°) and b) E-plane (φ=90°) vs. frequency for the optimised double layer LWA excited by a unit amplitude electric line source located at z_2.

III. Finite-Size Model and Experimental Results

The optimized double-layer PRS LWA was simulated in CST Microstripes™ considering a finite lateral size with dimension 28 x 28 cm^2, i.e. just over 13λ, which allows to minimize edge effects. Simulations of the performance of the feeding source were also carried out. Initially, the cavity was fed by a 3mm long thin wire model dipole located parallel to the *y*-axis and at $h_r/2$ in order to validate the design method presented in this paper. Subsequently, an accurate simulation model for a practical dipole source was constructed. The cavity was fed by a 2 mm semi-ridged co-axial cable inserted through a drill hole in the ground plane. The hole punctures the ground plane at the centre and the coaxial goes through to the middle of the cavity formed between the lower PRS and the ground plane. For the purpose of these simulations the outer shield of the co-axial cable was insulated from the metallic ground plane. Simulations carried out indicate that soldering the outer shield of the co-axial cable to the ground plane alters the radiation patterns obtained. The inner conductor of the coaxial, with dimensions 0.455 mm, is extended to the middle of the cavity (e.g. z=h_r/2= 5.45 mm) and bent parallel to the plane of the antenna (XY-plane in Fig. 1).

The gain at boresight as obtained using Periodic MoM-reciprocity as well as CST MS™ with the ideal wire dipole model and the coaxial monopole feed is shown in Fig. 8. A very good agreement is observed between the design technique (dash blue line) and the finite antenna fed by the ideal wire dipole model (black line) along the whole frequency band. The agreement with the coaxially fed finite antenna (grey line with dot marker) is fairly good at the centre and upper frequency band; however, we observe a disagreement at lower frequencies. This effect was further studied concluding that the vertical currents flowing on the inner coaxial that fed the "realistic" dipole affect the mode excitation in the cavity. In particular, at low frequencies ($f<f_{odd}$) a *TM mode* which is a perturbation of the quasi-static TEM mode of a parallel-plate waveguide is excited in the cavity due to the currents on the inner coaxial wire section perpendicular to the ground plane. As a result, the total radiated power at low frequencies increases (red dash line with star marker in Fig. 8) which leads to lower directivity values and therefore lower values of the gain. In the case of the ideal *y*-polarised dipole excitation, this mode is not excited P_{rad} (red dash line in Fig. 8) and remains low at lower frequencies. It is noted that the antenna radiation efficiency is between 84-89% within the frequency band of interest. Losses are mainly due to the FR4 substrates.

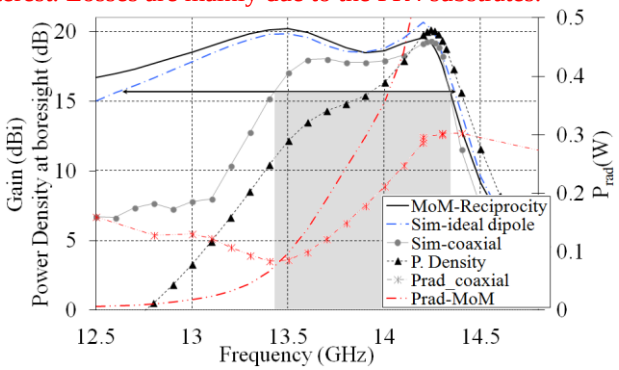

Fig. 8 Gain, radiated power density and total radiated power at boresight of the optimised double layer square patch PRS cavity antenna, as obtained using Periodic MoM-reciprocity and CST Microstripes™ 2009 with an ideal dipole feed and a coaxial fed dipole.

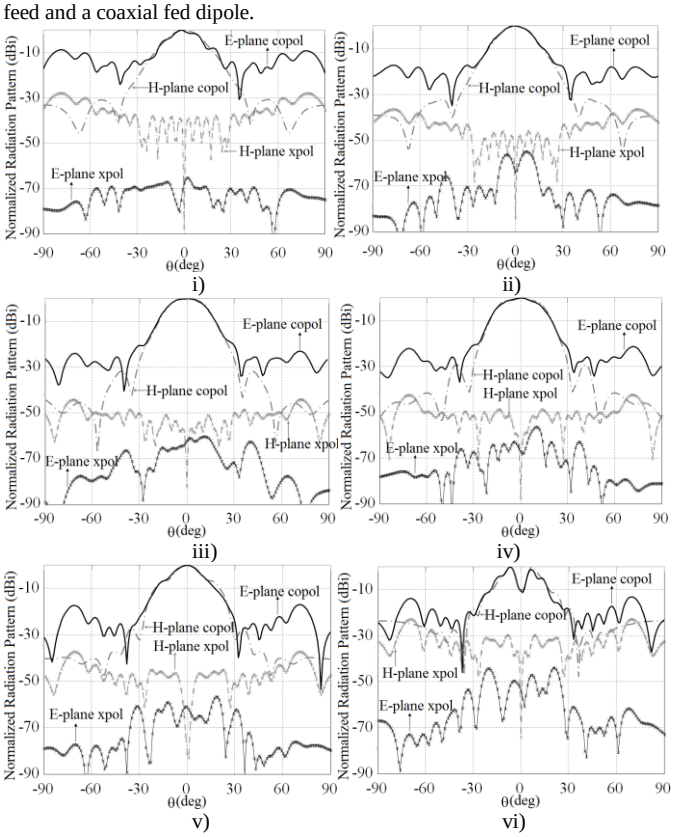

Fig. 9 Simulated E- and H-plane radiation pattern at i) 13.2 GHz, ii) 13.4 GHz, iii) 13.7 GHz, iv) 13.9GHz, v) 14.3GHz and vi) 14.4GHz for the antenna of Fig. 4 which was fed by a bent coaxial monopole.

A. *Directivity Bandwidth Characteristics*

The simulated H- and E- plane radiation patterns for the antenna fed by a coaxial monopole are shown in Fig. 9 between 13.2 and 14.4GHz. At low frequencies outside the operating band, i.e. at 13.2GHz, the patterns are distorted and high Side Lobe Levels (SLL) are observed. This is mainly due to the *TM mode* excited by the feeding source. Between 13.4 and 14.3GHz (i.e. frequencies within the 3dB bandwidth – shaded area in Fig. 8) a broadside pencil beam is obtained across the band with a SLL lower than 20dB and 30dB in the E and H-plane respectively. Higher SLL are observed in the E-plane due to the spurious radiation of the unwanted *TM mode* which could not be predicted in the diagrams of Fig. 7 as an ideal source was considered. At 14.2GHz the even leaky mode starts radiating at broadside and both modes coexist in the antenna. At higher frequencies, i.e. 14.4 GHz, the even leaky mode is already in the scanning region as predicted in Fig. 7, which creates a conical scanned beam, as expected from bi-directional LWAs, and the SLL increases due to radiation from higher order leaky-wave modes. The cross-polarization level is lower than -30dB for both planes.

B. *Experimental measurements*

The wideband LWA has been manufactured. The patches of each layer were etched on FR-4 substrates. The two layers were separated by an air cavity and attached to each other by the use of four plastic screws placed in the four corners of the dielectric boards and four at the central part of each side. Plastic spacers were also used to keep the boards parallel and at the specified distances above each other (dimension S= 10.1mm), as shown in Fig. 10. The antenna has been formed using the double-layer PRS attached to a ground plane by the use of the same plastic screws and plastic spacers placed in the four corners of the metallic ground plane board, 28 x 28 cm^2, and at the central point of each side. A central monopole manufactured by bending the inner connector of a semi-rigid coaxial cable was used as a feeding source. Limitations in the accuracy of the measurements mainly relate to the alignment of the PRSs and/or the flatness across the lateral dimension of the FR-4 boards. As shown in the parametric study of Section II, distances are critical. Therefore, it is essential that S and more importantly h_r are accurate since they will determine the level of excitation and frequency at which odd and even modes will be excited. For this reason, in the measurements the resonant distance, h_r, was slightly altered to 10.2 mm due to the boards being slightly bowed at the centre.

The gain and the radiation patterns of the antenna were measured in an anechoic chamber. The measurement set-up is presented in Fig. 10 with a detailed description of the source employed. The dynamic range of the measurements was -35dB. The gain and return loss of the transmitting antenna was measured and are depicted in Fig. 10, together with the simulation results. As can be observed, high gain is obtained between 13.4 GHz and 14.1 GHz, with a maximum value of 17.44dBi. The simulated input reflection coefficient is smaller than -6dB within the frequency band of interest with a minimum of -31dB at 14GHz. The measured input reflection coefficient is even lower at the lower end of the operating band and remains well below -10dB across the band. This indicates that reflection losses are very minor. The disagreement at the second maximum (f=14.1 GHz) was due to the misalignment of the PRSs which caused the antenna to radiate its maximum at a different angle (not at θ=0 as shown here). This can be observed in Fig. 11c (H-plane). The 3dB fractional bandwidth is approximately 6%.

The H- and E- plane radiation patterns were measured for the antenna at three different frequencies within the frequency band and are shown in Fig. 11. Good agreement between simulation results using CST MS^{TM} and measurements is observed. The SLL remains lower than -20 dB in the H-plane and E-plane within the frequency band. The cross polarization level has been measured and is below -28 dB throughout the frequency range studied.

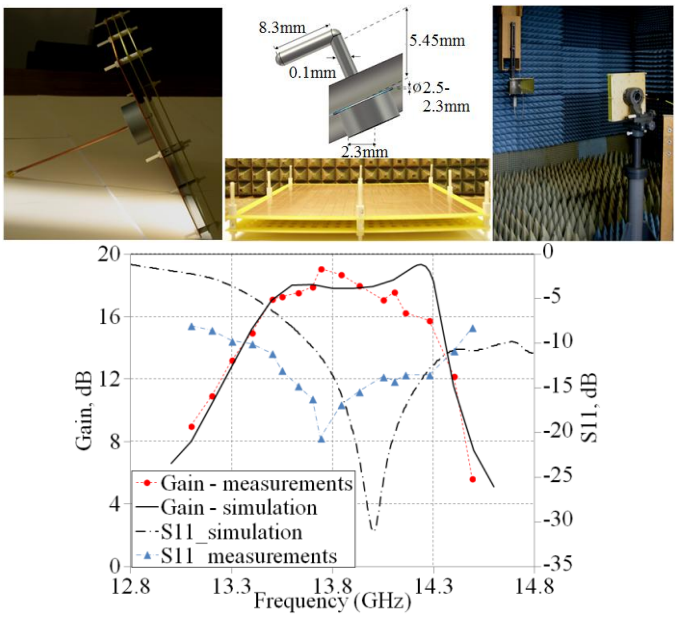

Fig. 10 Photographs of the antenna prototype, feeding sketch and measurements set-up. Measured and simulated gain and return loss.

IV. CONCLUSIONS

A rigorous analysis and design of broadband highly directive FP LWAs employing an optimised double-layer PRS has been presented using periodic MoM together with reciprocity. The technique is fast and accurate for the design of the proposed antennas. An analysis of the field distribution in the cavities formed between the PRS layers and the ground plane has demonstrated the excitation of a parallel (even) and antiparallel (odd) mode within the antenna operating frequency band. The effect of the PRS element dimensions and the thickness of the cavities on the two excited modes have been rigorously studied. Design guidelines for optimising the bandwidth of these antennas have been presented yielding an antenna design with bandwidth six times wider than that obtained by a single array LWA with the same directivity. The results have been validated using a 3D full-wave electromagnetic simulator. An antenna prototype has been fabricated and experimentally tested, validating the accuracy of the design technique. Future work will be directed towards a deterministic design of multilayer FP antennas using coupled-resonant-cavity theory. The limitations in the maximum attainable bandwidth-gain product of multi-layer FP antennas can be assessed using the proposed design approach.

REFERENCES

[1] A. Oliner. "Leaky-wave antennas," in Antenna Engineering Handbook, Third Ed., edited by *R. C. Johnson, McGraw Hill*, Chap. 10, 1993.

[2] C. Caloz, T. Itoh, "Electromagnetic Metamaterials: transmission line theory and microwave applications," *John Wiley & Sons, Inc.*, 2006.

[3] J. R. James, and P. S. Hall, "Handbook of microstrip antennas," *Peter Peregrinus Ltd.*, 1989.

[4] D. R. Jackson and N. G. Alexopoulos "Gain enhancement methods for printed circuit antennas", *IEEE Trans. Antennas Propagat.*, vol. AP-33, pp.976 -987, Sep. 1985.

[5] H. Y. Yang and N. G. Alexopoulos "Gain enhancement methods for printed circuits antennas through multiple substrates", *IEEE Trans. Antennas Propag.*, vol. 35, no. 7, pp.860 -863, Jul. 1987.

[6] D. R. Jackson, A. A. Oliner, and A. Ip, "Leaky-wave propagation and radiation for a narrow-beam multiple-layer dielectric structure," *IEEE Trans. Antennas Propag.*, vol. AP-41, pp. 344-348, Mar. 1993.

[7] M. Thévenot, C. Cheype, A. Reneix, and B. Jecko, "Directive photonic band gap antennas," *IEEE Trans. Microwave Theory Tech.*, vol. 47, pp. 2115, Nov. 1999.

[8] T. Zhao, D. R. Jackson, J. T. Williams, and A. A. Oliner, "Simple CAD model for a dielectric leaky-wave antenna," *IEEE Antennas Wireless Propag. Lett.*, vol. 3, pp. 243-245, April 2004.

[9] G.V. Trentini, "Partially reflecting sheet array", *IRE Trans. Antennas Propag.*, vol. AP-4, pp. 666-671, 1956.

[10] A. P. Feresidis, and J. C. Vardaxoglou, "High-gain planar antenna using optimized partially reflective surfaces," *Proc. Inst. Elect. Microw. Antennas Propag.*, vol. 148, no. 6, Feb. 2001.

[11] Y. J. Lee, J. Yeo, R. Mittra, and W. S. Park, "Design of a high-directivity electromagnetic bandgap (EBG) resonator antenna using a frequency selective surface (FSS) superstrate," *Microw. Opt. Technol. Lett.*, vol. 43, no. 6, 462-467, Dec. 2004.

[12] T. Zhao, D. R. Jackson, J. T. Williams, Hung-Yu D. Yang, and A. A. Oliner, "2-D Periodic Leaky-Wave Antennas-Part I: Metal Patch Design," *IEEE Trans. Antennas Propag.*, vol. 53, no. 11, pp.3505-3514, Nov. 2005.

[13] T. Zhao, D. R. Jackson, J. T. Williams, Hung-Yu D. Yang, and A. A. Oliner, "2-D Periodic Leaky-Wave Antennas-Part II: Slot Design", *IEEE Trans. Antennas and Propag.*, vol. 53, no. 11, pp. 3515-3524, Nov. 2005.

[14] A. P. Feresidis , G. Goussetis , S. Wang and J. C. Vardaxoglou "Artificial magnetic conductor surfaces and their application to low-profile high-gain planar antennas", *IEEE Trans. Antennas Propag.*, vol. 53, no. 1, pp. 209 -215, Jan. 2005.

[15] S. Wang, A.P. Feresidis, G. Goussetis, and J.C. Vardaxoglou, "High-Gain Subwavelength Resonant Cavity Antennas Based on Metamaterial Ground Planes," *Proc. Inst. Elect. Microw. Antennas Propag.*, vol. 153, no. 1, pp.1 -6, Feb. 2006.

[16] J. R. Kelly, T. Kokkinos, and A. P. Feresidis, "Analysis and Design of Sub-wavelength Resonant Cavity Type 2-D Leaky-Wave Antennas," *IEEE Trans. Antennas and Propagation*, vol. 56, no. 9, pp. 2817-2825, Sept. 2008.

[17] D. Sievenpiper, Z. Lijun, R.F. Broas, N.G. Alexopoulos and E. Yablonovitch, "High-impedance electromagnetic surfaces with a forbidden frequency band," *IEEE Trans. MTT*, vol. 47, no. 11, pp. 2059-2074, Nov. 1999.

[18] L. Leger, T. Monediere, and B. Jecko, "Enhancement of gain and radiation bandwidth for a planar 1-D EBG antenna," *IEEE Microw. Wireless Components Lett.*, vol. 15, no. 9, pp. 573–575, Sep. 2005.

[19] R. Gardelli, M. Albani, and F. Capolino, "Array thinning by using antennas in a Fabry-Perot cavity for gain enhancement", *IEEE Trans. Antennas Propag.*, vol. 54, no 7, pp. 1979 -1990, July 2006.

[20] A.R. Weily, K.P. Esselle, T.S. Bird, and B.C. Sanders, "Dual resonator 1-D EBG antenna with slot array feed for improved radiation bandwidth" *Proc. Inst. Elect. Microw. Antennas Propag., vol. 1, no. 1, pp.198 -203*, Feb. 2007.

[21] Z.-G. Liu, W.-X. Zhang, D.-L. Fu, Y.-Y. Gu, and Z.-C. Ge, "Broadband Fabry-Perot resonator printed antennas using FSS superstrate with dissimilar size," *Microw. Opt. Technol. Lett.*, vol. 50, no. 6, pp. 1623–1627, June 2008.

[22] J. Yeo, and D. Kim, "Novel design of a high-gain and wideband Fabry-Pérot cavity antenna using a tapered AMC substrate," J Infrared Milli. Terahz. Waves, vol.30, pp.217–224, Jan. 2009.

[23] A. P. Feresidis, J. C. Vardaxoglou, **"**A broadband high-gain resonant cavity antenna with single feed", *Proc. EuCAP\'06*, Nice, France, 2006.

[24] L. Moustafa and B. Jecko, "EBG structure with wide defect band for broadband cavity antenna applications," *IEEE Antenna Wireless Propagat. Lett.*, vol.7, pp.693-696, Nov.2008.

[25] S.A. Hossseini, F. Capolino, and F.D. Flaviis, "A new formula for the pattern bandwidth of Fabry Pérot cavity antennas covered by thin frequency selective surfaces," *IEEE Trans. Antennas Propag*., vol. 59, no. 7, pp. 2724-2727, Jul. 2011.

[26] S. A. Muhammad, R. Sauleau, and H. Legay "Small-Size Shielded Metallic Stacked Fabry–Perot Cavity Antennas With Large Bandwidth for Space Applications," *IEEE Trans. Antennas Propag.*, vol. 60, pp. 792-802, Feb. 2012.

[27] Ge Yuehe, K.P. Esselle, and T.S. Bird, "The Use of Simple Thin Partially Reflective Surfaces With Positive Reflection Phase Gradients to Design Wideband, Low-Profile EBG Resonator Antennas ", *IEEE Trans. Antennas Propag.*, vol. 60, no. 2, pp. 743 - 750, Feb. 2012.

[28] C. Mateo-Segura, A.P. Feresidis, and G. Goussetis, "Highly directive 2-D leaky wave antennas based on double-layer meta-surfaces," *Proc. EuCAP\'10*, pp.1-5, April 2010.

[29] C. Mateo-Segura, A.P. Feresidis, and G. Goussetis, "Analysis of broadband highly-directive Fabry-Perot cavity Leaky-Wave antennas with two periodic layers," *IEEE Int. Antennas Propag. Symp. Dig.*, pp. 1 – 4, July 2010.

[30] C. Mateo-Segura, A.P. Feresidis, and G. Goussetis, "Broadband Leaky-Wave Antennas with double-layer PRS: Analysis and design," *Proc. EuCAP\'11*, pp. 2102-2105, 11-15 April 2011.

[31] R. Mittra, C.H. Chan, T. Cwik, "Techniques for analyzing frequency selective surfaces-a review," *Proceedings of the IEEE*, vol. 76, pp.593-615, Dec. 1988.

[32] C. Mateo-Segura, *G.* Goussetis, and A. P. Feresidis, "Sub-wavelength Profile 2-D Leaky-Wave Antennas with Two Periodic Layers", *IEEE Trans. Antennas Propag.*, vol. 59, pp.416- 424, Feb. 2011.

[33] J-S. Hong and M.J. Lancaster, "Microstrip Filters for RF/Microwave Applications," *Wiley-Interscience*, 2001.

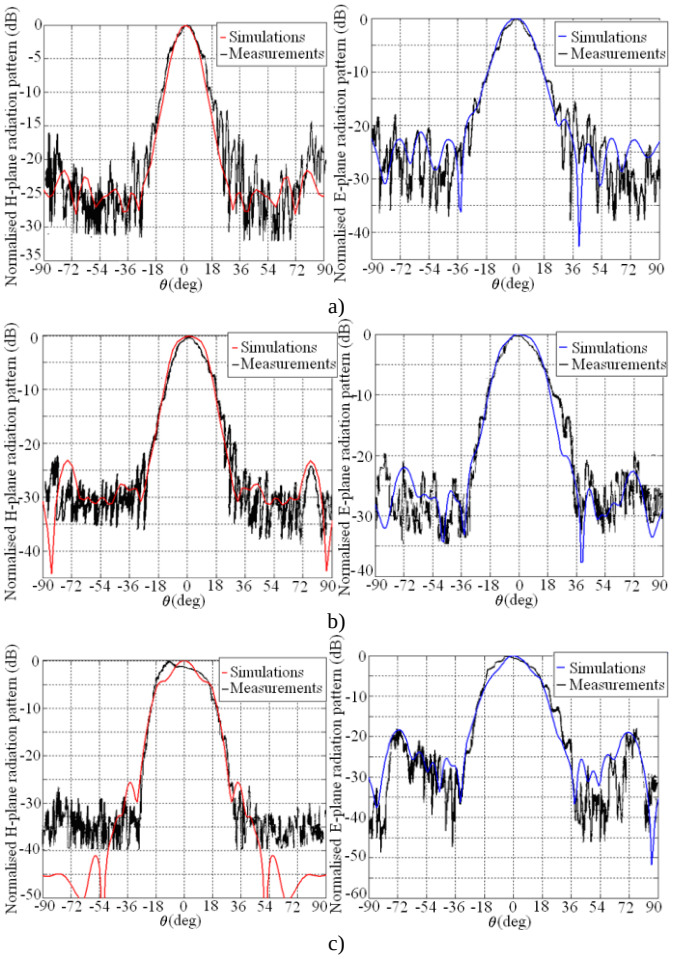

Fig. 11 Measured H-plane (red plots) and E-plane (blue plots) radiation pattern at a) 13.5 GHz, b) 13.9 GHz and c) 14.1 GHz.